Available online at www.sciencedirect.com

ScienceDirect

Polar Science 8 (2014) 315–326

http://ees.elsevier.com/polar/

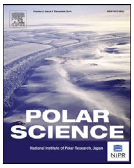

Development of a cloud detection method from whole-sky color images

Masanori Yabuki [a,*], Masataka Shiobara [b,c], Kimiko Nishinaka [d], Makoto Kuji [d]

[a] *Research Institute for Sustainable Humanosphere, Kyoto University, Uji, Kyoto 611–0011, Japan*
[b] *National Institute of Polar Research, Tachikawa Tokyo 190–8518, Japan*
[c] *Department of Polar Science, The Graduate University for Advanced Studies, Tachikawa, Tokyo 190-8518, Japan*
[d] *Nara Women's University, Nara, Nara 630–8506, Japan*

Received 15 January 2014; revised 5 June 2014; accepted 18 July 2014
Available online 7 August 2014

Abstract

A method is proposed for detecting clouds from whole-sky color images obtained with an all-sky camera (ASC) system. In polar regions, cloud detection using whole-sky images usually suffers from large uncertainties in fractional cloud cover retrievals because of large solar zenith angles (SZAs) and high surface albedo, which cause "whitening" in the images. These problems are addressed by using differences between real images and virtual clear-sky images for a particular observation time with the same SZA. The method is applied to ASC images obtained at Ny-Ålesund, Svalbard in May of 2005–2007, and the results are compared with Micro-Pulse Lidar (MPL) measurements. When no clouds were detected by MPL, the false cloud detection rate from ASC classification was 2.1% in total hours. Conversely, when clouds were detected by MPL, the ASC classification underestimated the clouds by 11.6%. In most cases, this occurred when MPL detected very optically thin clouds. Furthermore, the variability of cloud fractions estimated by MPL and ASC was roughly constant regardless of the SZA. Thus, it is confirmed that the method developed in this study is valid for cloud detection from whole-sky color images.

Keywords: Cloud detection; Whole-sky image; All-sky camera; Micro-pulse lidar

1. Introduction

Clouds play a key role in the earth's radiation budget, by reflecting incoming solar radiation and trapping outgoing radiation. Analyses of satellite remote sensing data indicate that, in polar regions, the warming effect of clouds is larger than the cooling effect; however, the opposite is true in mid- and lower latitudes (Hartmann, 1993). However, passive satellite sensors cannot accurately identify clouds over polar regions, which hampers the investigation of the effects of clouds on the radiation budget (Raschke et al., 2005). Recently, space-borne and ground-based active remote sensors such as radar and lidar have revealed detailed vertical profiles of ice and water clouds, and have been used to investigate profiles of radiative heating rate (e.g., Thorsen et al., 2013). Active remote sensors can only provide detailed vertical profiles at nadir or zenith, but stratiform clouds such as Arctic

---

* Corresponding author.
E-mail address: yabuki@rish.kyoto-u.ac.jp (M. Yabuki).

http://dx.doi.org/10.1016/j.polar.2014.07.004
1873-9652/

stratus clouds can extend over several hundreds of kilometers. Therefore, optical imaging sensors should be used in combination with active sensors to monitor extended cloud systems, because the amount and altitude of clouds are key properties for determining the magnitude of radiative effects.

Whole-sky imaging is more useful than zenith observations for cloud determination, because the field of view of the sky camera corresponds to the conventional sky-type observations of meteorological observers. Ground-based sky imaging systems have commonly been used to obtain continuous information about cloud distributions by measuring sky radiance at visible and/or near infrared wavelengths (e.g., Shields et al., 1998, 2013; Feister et al., 2010; Liu et al., 2013). Recently, new methodologies have led to improvements in cloud classification. Heinle et al. (2010) constructed an automatic cloud classification algorithm based on a set of mainly statistical features describing the color and texture of an image. This algorithm employs the k-nearest-neighbor classifier, because of its high performance, simplicity of implementation, and low computational complexity. Heinle et al. (2010) distinguished between seven different sky conditions: high thin clouds (cirrus and cirrostratus), high patchy cumuliform clouds (cirrocumulus and altocumulus), stratocumulus clouds, low cumuliform clouds, thick clouds (cumulonimbus and nimbostratus), stratiform clouds, and clear sky. An improved cloud classification algorithm, based on the work of Heinle et al. (2010), which includes a metric for the existence of rain in digital images, was developed and demonstrated by Kazantzidis et al. (2012).

In this paper, we focus on daytime color whole-sky images divided into three components: red, green, and blue. In general, cloud detection methods are valid for whole-sky images with a high color contrast between a clear sky and clouds. In most cases, image processing algorithms have been developed to estimate cloud fractions by reasoning that the ratio or difference between red and blue color intensities reflects differences in the wavelength dependence of the scattered light between air molecules and clouds (e.g., Long et al., 2006; Heinle et al., 2010). However, Long et al. (2006) stated that using a unique threshold of the red—blue ratio can result in problems with, for example, misdetection of thin clouds in circumsolar pixels in high aerosol conditions. Such pixels are often whiter and brighter than the rest of the hemisphere because of forward scattering by aerosols and haze. Kazantzidis et al. (2012) reported that the use of a red—blue intensity ratio or difference results in errors for cases of broken cloud or overcast conditions at large solar zenith angles (SZAs). They proposed a multi-color threshold that also takes into account the green intensity of the image for discriminating cloud areas. Alonso et al. (2014) used direct normal irradiance to correctly identify the solar disk, to resolve the problem related to the saturation of pixels in images from sky cameras being used to detect clouds.

In polar regions, cloud detection using whole-sky images usually suffers from large uncertainties because of the large SZAs, as well as the high surface albedo, which causes “whitening” of the images. In this study, we propose a semi-empirical technique that detects clouds by comparing an observation with a virtual clear-sky image at the appropriate sun elevation constructed from a database of real clear-sky images. Using the clear-sky image, we can take into account the inhomogeneity of the sky radiance distribution, and reduce errors that arise from the degradation of Charge Coupled Device (CCD) cameras. Our detection method allows the classification of sky types using red—green—blue (RGB) spectral features. We applied our detection method to images obtained with an all-sky camera system at Ny-Ålesund in May for the years 2005—2007. We then compared the detected clouds with cloud measurements using a Micro-Pulse Lidar (MPL) system. In this paper, we describe the details of this procedure and demonstrate the effectiveness of the proposed method.

2. Instrumentation

We used the PSV-100 All-Sky Camera (ASC) system manufactured by Prede Co., Ltd., Japan, to obtain whole-sky color images. The PSV-100 model consists of an all-sky camera unit with a blade (a device to shield from direct sunlight). In the camera unit, a fisheye lens is mounted on a camera that has a field of view of up to 160°. The image sensor is a 1/3″ type color CCD, adjusted for daylight. The whole-sky images were taken at 10-min intervals, and saved in an 8-bit JPEG format with a maximum of 380,000 pixels. The blade to block off direct sunlight rotates automatically to track the solar orientation, which was calculated from the observation time, longitude, and latitude. It was necessary to analyze an average of 3 × 3 pixels to take into account the variations in pixel intensity when detecting optically thin clouds. For classification of the sky types in this paper, we used the 2086 hourly images (93.5% in total hours) observed at Ny-Ålesund during May of 2005—2007.